OPTOELECTRONICS AND ADVANCED MATERIALS – RAPID COMMUNICATIONS Vol. 1, No. 12, December 2007, p. 663 - 666

Sb_xSe_{100-x} system ($0 \leq x \leq 8$) studied by DSC and Raman spectroscopy

J. HOLUBOVÁ*, Z. ČERNOŠEK, E. ČERNOŠKOVÁ[a]
Department of General and Inorganic Chemistry, University of Pardubice, nám. Legii 565, CZ-532 10 Pardubice, Czech Republic
[a]*Joint Laboratory of Solid State Chemistry of Institute of Macromolecular Chemistry of Czech Academy of Sciences and University of Pardubice, Studentská 84, CZ-532 10 Pardubice, Czech Republic*

The Sb_xSe_{100-x} glass-forming system (x = 0, 1, 2, 4, and 8 at. %) was studied by conventional differential scanning calorimetry (DSC), Step Scan DSC and Raman spectroscopy. Glass transition temperature, T_g, as well as isobaric heat capacity change, ΔC_p, were determined. Crystallization of Sb_2Se_3 from incongruent undercooled melt, followed by trigonal selenium crystallization was observed. The crystallization kinetics of Sb_2Se_3 was studied in details. Sb_2Se_3 crystallizes from incongruent melt at T_c = 107±2 °C with crystallization enthalpy $\Delta H_c(Sb_2Se_3)$ = -52± J/g. Johnson-Mehl-Avrami kinetics of crystallization with Avrami kinetic exponent close to 3 was found.

(Received October 25, 2007; accepted November 22, 2007)

Keywords: DSC, StepScan DSC, Raman spectroscopy, Selenium, Sb-Se system, Glass transition, Crystallization

1. Introduction

One of the interesting properties of chalcogenide glasses is that they exhibit a wide spectrum of photoinduced effects. Owing to this fact the possibility of application of these materials in electronics and optoelectronics arises, e.g. optical memories, photoresists, X-ray imaging etc. Especially amorphous selenium had evoked much interest from application point of view in the past decades [1]. However, there are some shortcomings of pure selenium for its practical application including low sensitivity and thermal stability, short lifetime and low hardness. It was found that these inadequate properties can be improved by alloying of some elements to selenium matrix as it is for example the elements from V. B group of periodic table arsenic and antimony.

Considerable attention has been paid to glasses of Sb-Se as these materials have greater hardness and greater electric conductivity in comparison with pure selenium, see e.g. [2]. Glasses of this system have been studied from the viewpoint of their desirable recording properties; these materials can be used as data storage material on the base of change amorphous phase - crystal phase [3]. However, the application of Sb containing glasses is limited by their considerable tendency to crystallization. The proper description of thermal behavior of these glasses is important for understanding their properties and applications, but the glasses of this system are not enough studied probably due to considerable difficulties in their preparation. Some previous studies concerning glass transition, stability and crystallization of undercooled melts have been carried out by conventional DSC [4,5] and temperature modulated differential scanning calorimetry (MDSC) [6].

As far as Raman spectra of system studied are concerned no relevant information are available in literature and only a little information of Sb_2Se_3 Raman spectra can be found [7].

The aim of this work is to study the thermal properties and the structure of selenium based glasses with small amounts of antimony (1 - 8 at. %) by conventional DSC, StepScan DSC and Raman spectroscopy.

2. Experimental

The glasses of Sb_xSe_{100-x} system (x = 1, 2, 4 and 8 at. %) were prepared by conventional direct synthesis (melt-quenching technique) from pure elements of 5N purity. Synthesis was done in evacuated quartz ampoules in horizontal rocking furnace. The ampoules were exposed to a temperature 900 °C for 12 hours and after synthesis they were quickly cooled down in cold water. Both homogeneity and composition were controlled using X-ray fluorescence (XRF) analyzer Eagle II (Roentgen Messtechnik AG). Glassy selenium were prepared by melting of high purity selenium at evacuated quartz ampoules at 850 °C for 2 hours and subsequently cooled at air.

The DSC experiments were performed on differential scanning calorimeter Pyris 1 (Perkin-Elmer). The heating rates used for the conventional DSC were q = 5, 10, 12.5, 15 and 20 K/min. In addition to conventional DSC measurement the StepScan DSC method was used. This method allows separating fast reversible processes from slow kinetic ones and thus two curves are obtained as the output. The reversible part corresponds to temperature change of the isobaric heat capacity (the change of vibrational amplitude) and irreversible or kinetic heat flow reflects processes with long relaxation times, e.g. structural relaxation and crystallization. The measurement proceeds in repeated steps. In every step the temperature firstly changes and then the isotherm of variable length follows. The typical result of StepScan DSC is in Fig. 1.

The measurements were carried out in heating scans for each composition. A typical sample weight was 10 mg, they were sealed in standard aluminium pans and scanned over a temperature range 30 – 250 °C at the temperature step 1 °C and step heating rate 10 K/min. The maximal difference of heating flow allowed at the end of isotherm was $\Delta Q = \pm 0.0001$ mW.

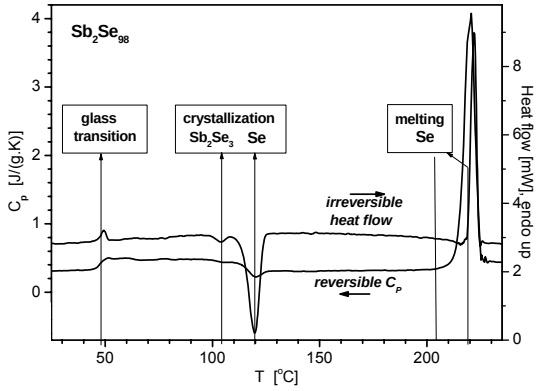

Fig. 1. Typical results obtained by StepScan DSC.

Raman spectra (resolution 2 cm^{-1}) were taken using FT-IR spectrometer Bruker IFS 55 with Raman accessory FRA 106, Ge detector and Nd:YAG excitation laser (1064 nm).

3. Results and discussion

3.1 DSC measurements

The glass transition temperature was determined for every composition. To avoid kinetic effects related to thermal history the glass transition temperature was measured by StepScan DSC, for more details see [8-10]. Glass transition temperature changed by 8 °C over the whole compositional range achieving maximum for glass containing 4 at.% Sb. The isobaric heat capacity change at glass transition, ΔC_P, changed slightly up to 4 at.% Sb and then decreased for 8 at.% Sb, Fig. 2.

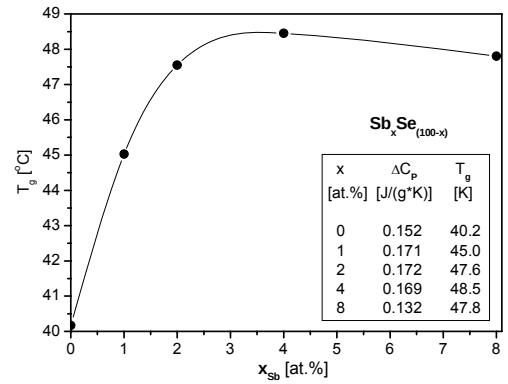

Fig. 2. Compositional dependence of glass transition temperature obtained by StepScan DSC. The line is only a guide for the eye. Characteristic values of glass transition are listed in the inset.

Non-isothermal crystallization of glasses was also studied. Using conventional DSC (heating rate 5 K/min) two crystallization peaks at 116 - 122 °C and 179 - 183 °C, respectively, and one melting peak at 222 °C were found. For Sb_1Se_{99} composition the first crystallization peak was poorly distinguishable and its resolution gradually improved with increasing content of Sb. At the same time both crystallization peaks slightly moved to higher temperatures. Temperature of melting peak remained unchanged.

Samples were heated up to 250 °C, sufficiently high above the selenium melting temperature and than cooled down to room temperature with rate -100 K/min and measured once more. In the second heating scan glass transition temperature decreased to T_g of selenium, the first crystallization peak didn't appear and only the second crystallization and melting peaks were observed again. As melting temperature of Sb_2Se_3 is 611 °C, we can suppose that the first crystallization peak can be related to the crystallization of Sb_2Se_3 from glassy matrix and the second one, as well as the melting peak, can be assigned to the crystallization and melting of selenium, respectively.

Crystallization was also studied by StepScan DSC. Because of step-like method with very slow underlying heating rate these measurements can be assumed like quasi-isothermal. As one can expect, contrary to conventional DSC, both markedly narrower crystallization peaks were found at lower temperatures, Fig. 1, and their peak positions dependence on antimony content was negligible. Results observed can be easily explained as considerable suppression of influence of crystallization kinetics on StepScan DSC records, especially in the case of selenium crystallization.

The crystallization enthalpy of the low temperature peak depends almost linearly on Sb content, see Fig. 3, except of sample containing 8 at.% Sb where lower crystallization enthalpy was found. Using both experimentally found enthalpy (10.1 J/g) and enthalpy determined from linear extrapolation (12.3 J/g), it is possible to estimate that of about 8 wt.% of Sb_8Se_{92} sample was already crystallized like Sb_2Se_3 during preparation.

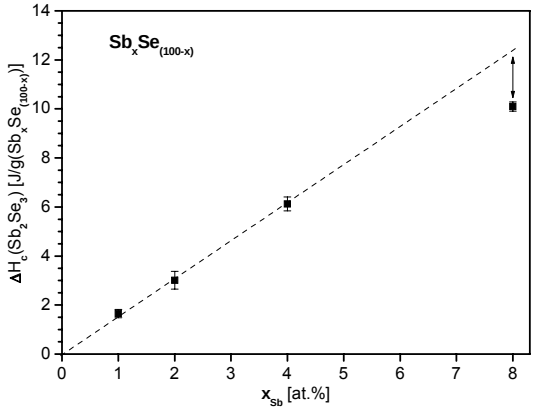

Fig. 3. The compositional dependence of crystallization enthalpy of Sb_2Se_3 crystallized from 1 g of Sb_xS_{100-x} incongruent melt.

Using quasi-isothermal StepScanDSC results for all composition under study, crystallization enthalpies of Sb_2Se_3 (first crystallization peak) were recalculated on the Sb_2Se_3 weight content in samples of formal formula $(Sb_2Se_3)_x.Se_{(100-x)}$.

Crystallization enthalpy of Sb_2Se_3 crystallizing from incongruent melt with great overstoichiometry of selenium was found $\Delta H_c(Sb_2Se_3)$ = - 52 ± 2 J/g at crystallization temperature T_c = 107 ± 2 °C (crystallization peak temperature). It should be noted that crystallization enthalpy of Sb_8Se_{92} sample appointed from linear extrapolation (12.3 J/g) was used for calculation. Kinetics of Sb_2Se_3 crystallization is driven by Johnson-Mehl-Avrami (JMA) mechanism with kinetic exponent $n = 2.9 \pm 0.3$ and activation energy $E^* = 125 \pm 6$ kJ/mol. Because Sb_2Se_3 creates layered crystals, kinetic exponent close to 3 can be interpreted as simultaneous nucleation and two dimensional crystal growths [11].

Finally, using conventional DSC, Sb_8Se_{92} sample was measured up to 500 °C. Broad endothermic peak starting immediately after selenium melting and with flat maximum at approx. 400 °C was found, Fig. 4.

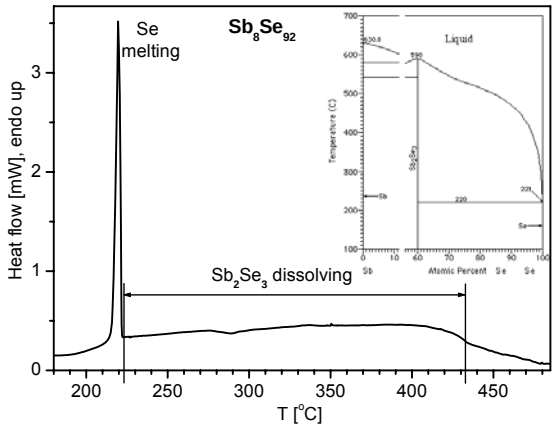

Fig. 4. Dissolving of Sb_2Se_3 crystals into selenium melt. Part of Sb-Se phase diagram is included. For details, see text.

In the sample of Sb_8Se_{92} composition up to 4.8 mol.% of crystalline Sb_2Se_3 can be created. Based on equilibrium phase diagram of Sb-Se system this broad peak could be related to dissolving of Sb_2Se_3 crystals in the selenium melt. Fact that experimentally observed end of dissolving is higher then this one found in equilibrium phase diagram (370 °C) reflects very probably the influence of non-isothermal dissolving kinetics recorded by DSC.

3.2 Raman spectroscopy

The glasses were further studied by Raman spectroscopy. Three characteristic vibrations were found at 112, 194 and 250 cm^{-1}, respectively, Fig. 5. The intensity of 194 cm^{-1} band increases with increasing antimony content and at the same time the intensity of 112 and 250 cm^{-1} band decreases. From it follows that the former band can be related to Sb-Se and the latter ones to Se-Se vibrations. The bands at 112 and 250 cm^{-1} are characteristic for Se-Se ring-like vibrations (*cis*-conformation) [12].

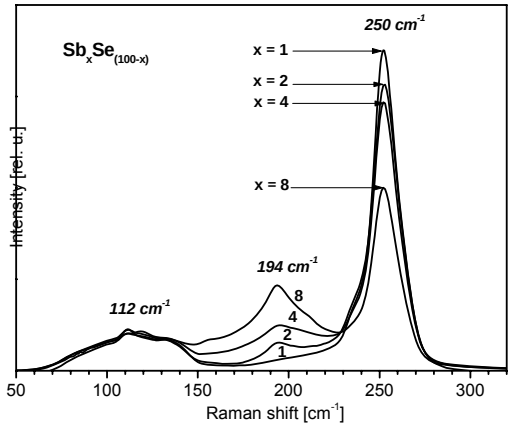

Fig. 5. Raman spectra of Sb_xSe_{100-x} bulk glasses.

The Sb_8Se_{92} sample were successively crystallized at temperature tightly above the first crystallization peak (115 °C) and at temperature fairly above second crystallization peak (205 °C) to ensure complete crystallization of sample. Raman spectra were recorded after each of crystallization, see Fig. 6. Sample crystallized above the temperature of Sb_2Se_3 crystallization is characterized by one intensive band at 192 cm^{-1}, that can be assigned to Se-Sb bond vibration, and doublet at 234 and 238 cm^{-1}. That doublet is characteristic for Se-chain vibration of trigonal selenium [12] but another characteristic vibration at 141 cm^{-1} is missing in the spectrum at the same time. We suppose that *cis*-conformation of selenium chains had to be changed to *trans*-conformation, typical for trigonal selenium, but trigonal selenium crystals were not still grown. After crystallization at 205 °C the intensity of doublet at 234 and 238 cm^{-1} rose up significantly and previously missing band at 141 cm^{-1} appeared, confirming the presence of trigonal selenium crystals, Fig. 6.

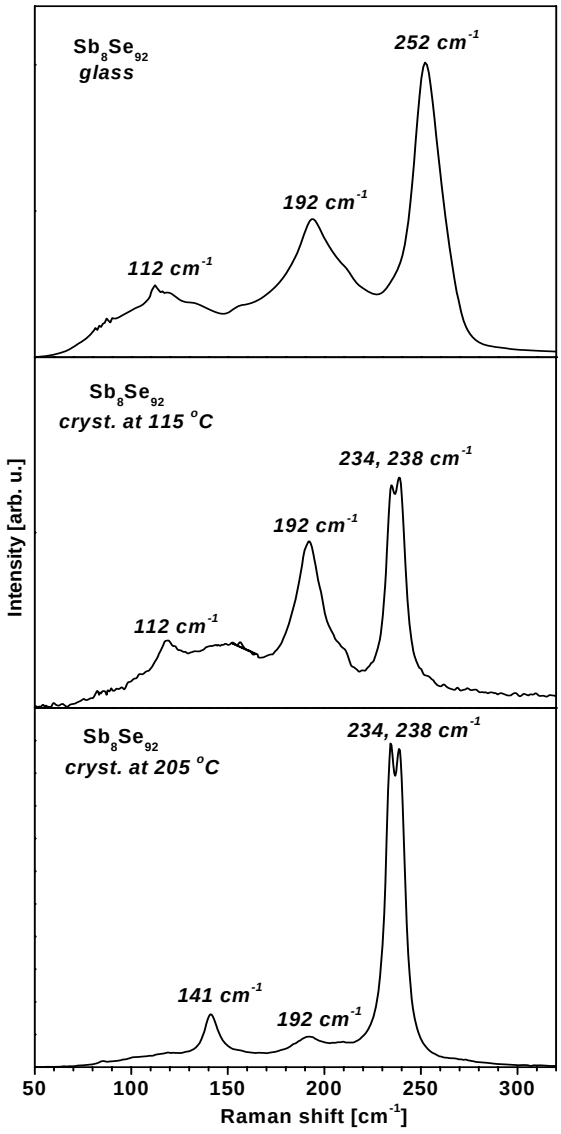

Fig. 6. Raman spectra of as-quenched Sb_8Se_{92} glass and after crystallization at marked temperatures. For details, see text.

Results obtained by Raman spectroscopy confirmed that the low-temperature DSC crystallization peak corresponds to the crystallization of antimony selenide and the higher one to the crystallization of selenium.

4. Conclusions

Thermal properties and structure of Sb_xSe_{100-x} glasses with low content of antimony (x = 1, 2, 4 and 8 at.%) were studied by conventional DSC, StepScan DSC and Raman spectroscopy. It was found that glass transition temperature as well as isobaric heat capacity change, ΔC_p, in the glass transition was changed with increasing antimony content with maximum for 4 at. % of Sb. We suppose that the decrease of both T_g and ΔC_p for Sb_8Se_{92} glass can be related to partial crystallization in the course of the glass preparation. That crystallization of Sb_8Se_{92} glass modifies the composition of glassy matrix leading to observed decreasing of T_g. The crystallization of undercooled melts was also studied and crystallization of Sb_2Se_3 from incongruent melt with great overstoichiometry of selenium, followed by selenium crystallization was observed. Crystallization of Sb_2Se_3 was studied in more details. Under quasi-isothermal conditions antimony selenide crystallizes at T_c = 107 ± 2 °C with crystallization enthalpy $\Delta H_c(Sb_2Se_3)$ = - 52 ± 2 J/g. Johnson-Mehl-Avrami kinetics of crystallization was found with Avrami kinetic exponent close to 3. Because of layered structure of Sb_2Se_3 crystals, this value means that nucleation and crystallization are in progress simultaneously.

According to Raman spectra it is possible to conclude: i) glassy matrix of bulk glasses is constituted mainly by selenium chains in *cis*-conformation (ring-like conformation); ii) antimony builds into selenium glassy matrix and the content of Sb-Se bonds increases along with increasing content of Sb (no characteristic vibrations of Sb-Sb bond were observed); iii) antimony selenide crystallizes firstly (it means at lower temperature) from incongruent undercooled melt and crystallization is completed by trigonal selenium crystals growth at higher temperature.

Acknowledgements

This work was supported by the project MSM 0021627501.

References

[1] K. Tanaka, Phys. Rev. **57**, 5163 (1998).
[2] G. Tonchev, B. Fogal, G. Belev, R. E. Johanson, S. O. Kasap, J. Non-Cryst. Solids **299-302**, 998 (2002).
[3] V. I. Mikla, I.P. Mikhalko, V.V. Mikla, Mat. Sci. Eng. **B83**, 74 (2001).
[4] N. Mehta, R. S. Tiwari, A. Kumar, Mat. Res. Bull. **41**, 1664 (2006).
[5] M. M. El-Zaidia, A. El-Shafi, A. A. Ammar, M. Abo-Ghazala, Thermochim. Acta **116**, 35 (1987).
[6] D. Tonchev, S. O. Kasap, J. Non-Cryst. Solids **248**, 28 (1999).
[7] J. Wang, Z. Deng, Y. Li: Mat. Res. Bull. **37**, 495 (2002).
[8] Z. Černošek, J. Holubová, E. Černošková, J. Optoelectron Adv. Mater. **4**, 489 (2002).
[9] J. Holubová, Z. Černošek, E. Černošková, J. Optoelectron Adv. Mater. **7**, 2671 (2005).
[10] Z. Černošek, J. Holubová, E. Černošková, Optoelectron Adv. Mater.-Rapid Commun. **1**, 277 (2007).
[11] D. W. Henderson, J. Therm. Anal. **15**, 325 (1979).
[12] G. Lucovsky, M. Mooradian, W. Taylor, G. B. Taylor, G. B. Wright, R. C. Keezer, Solid State Commun. **5**, 113 (1967).

*Corresponding author: jana.holubova@upce.cz